Multiband photometry of Geminga

V.G. Kurt[a], **V.N. Komarova**[b], **V.V. Sokolov**[b], **T.A. Fatkhullin**[b],
A.B. Koptsevich[c], **Yu.A. Shibanov**[c]

[a] Astro Space Centre of RAS, Moscow
[b] Special Astrophysical Observatory of the Russian AS, Nizhnij Arkhyz 369167, Russia
[c] Ioffe Physical Technical Institute, St.Petersburg

Abstract. We present the results of the BVRI photometry of the Geminga pulsar based on observations with the 6 m telescope. The Geminga magnitudes in B ($26^m1\pm0.5$), V ($25^m3\pm0.3$) and R_c ($25^m4\pm0.3$) are consistent with results of other studies of its optical emission in these spectral bands. We derive for the first time the magnitude in the I_c band to be $25^m1 \pm 0.4$, which is more than a magnitude higher if compared with the upper limit given in the paper of Mignani et al. (1998). The comparison of the broad-band spectra of this middle-aged isolated neutron star with the results of observations in the X-rays and hard ultraviolet suggests non-thermal origin of the Geminga emission at least in some bands of the visible range.

Key words: pulsars: photometry — pulsars: individual: Geminga

1. Introduction

Geminga is a unique representative of still not too numerous but a distinct subclass of isolated neutron stars (INS), with the emission being registered in a wide range of wavelengths. It was detected for the first time as a bright source of $\gamma-$radiation of unknown nature (Fichtel et al., 1975), which much more later was identified with a source of pulsed emission in the X-rays (Halpern & Holt, 1992). Regular pulsations of the same period of 0.237 ms were soon found in the $\gamma-$range, and Geminga was stated to be a neutron star like other pulsars. For a long time it has been considered "radio-quiet". The radio pulsar Geminga was discovered at rather low ($\lesssim$ 102.5 MHz) frequencies only (Kuz'min & Losovskii, 1997; Malofeev & Malov, 1997; Shitov & Pugachev, 1997). Unlike most of radio pulsars the pulse profile of Geminga is marginally unstable. The main parameters of the pulsar (Table 1) were estimated mainly via observations in the X and $\gamma-$rays.

Numerous observations of this neutron star with different telescopes (CFHT, ESO 3.6 m, NTT, 5 m Hale) yielded the identification of Geminga in the optical range and its multicolour photometry (Bignami et al., 1987; Halpern & Tytler, 1988; Bignami et al., 1996). In the course of studies with the *HST* the UV flux estimates were obtained, the Geminga proper motion and its annual parallax were derived, which allowed defining the distance to this object to be equal to $157\pm^{59}_{34}$ (Caraveo et al., 1996). The tentative detection of the pulsed optical emission of the Geminga is also worth mentioning (Shearer et al., 1998), but this needs to be confirmed.

In a wide range of wavelengths the Geminga spectrum is mostly non-thermal and is originated in the magnetosphere of the rotating neutron star. The only exception is the domain of the extremal UV and soft X-rays (0.1-2.4 keV) where the thermal emission from the surface of the cooling neutron star with a temperature $T \sim 5 \times 10^5$K (Halpern & Wang, 1997) dominates. The broad-band spectrum in the nearest UV range is close to the Rayleigh-Jeans part of the thermal one, detected in the soft X-rays. Analysis of the thermal emission and comparison of observations with the results of modeling of neutron star atmospheres and cooling simulations allow one to estimate the neutron star parameters (such as temperature and chemical composition of its surface, magnetic field, mass and radius, etc) and put constraints on properties of a superdense matter in the neutron star interiors (see, e.g., Yakovlev et al., 1999).

Studies of optical emission of middle-aged ($\tau \gtrsim 10^5$) INS such as Geminga and PSR B0656+14 are essential for more rigorous estimates of thermal component parameters and shedding light on the nature of non-thermal emission. Comparison with the same data for neutron stars of different ages and with theoretical predictions makes possible opting for more appropriate model of structure and evolution of these objects. The extremely low luminosity ($M_V \gtrsim 16$) strictly constrains studies of properties of optical emission of cooling INS. For being one of the closest

Table 1: *Geminga characteristics*

Coordinates,^{o}		P	$\dot{P} \times 10^{-15}$	τ	lgB	$lg\dot{E}$	d	DM
l	b	ms	s s^{-1}	yrs	G	erg s^{-1}	kpc	pc cm^{-3}
195.134	4.265	237	11	$3.4 \cdot 10^5$	12.20	34.51	~ 0.16	2.9

P – rotational period, characteristic age $\tau = P/(2\dot{P})$, magnetic field $B = 3.2 \times 10^{19}(P\dot{P})^{1/2}$, spin-down luminosity $\dot{E} = 4\pi^2 I \dot{P} P^{-3}$, inertia moment I is considerd to be 10^{45} g cm^2,
d – distance (Caraveo et al., 1996), DM – dispersion measure (Malofeev & Malov, 1997)

Table 2: *Observations of Geminga with the 6 m telescope*

Date	CCD detector	Filter	T_{exp}	Z	Seeing	Background
			s	deg		mag/$\square''$
11.03.97	ISD017A	R_c	3×600	31.9	$1''6$	20.80
12.03.97	ISD017A	V	3×600	27.7	$1''7$	21.29
13.03.97	ISD017A	B	5×600	32.8	$1''6$	21.47
		V	2×600	39.6	$1''6$	21.01
		R_c	600	41.5	$1''5$	20.44
20.10.98	ISD017A	I_c	13×300	31.9	$1''4$	18.89
19.01.99	Photometrics	R_c	300	26.2	$1''0$	20.38
		I_c	2×300	26.9	$1''0$	18.90
22.01.99	Photometrics	R_c	300	28.0	$1''9$	20.36
		V	600	28.7	$1''8$	21.24
		I_c	2×300	34.7	$2''0$	18.50

INS of middle age, Geminga is the most convenient for such an investigation. An amount of reliable data on its emission in a wide wavelength range has already been acquired.

Up to now the Geminga optical emission has not contradicted the model of thermal emission from the cooling neutron star surface. To explain the broad-band spectrum with excess at 6000Å and a dip in the I band (where the upper limit to the object flux was given only), the model of the ion cyclotron emission originated in the outer layers of the atmosphere of the neutron star with a magnetic field $B \sim 10^{12}$G was proposed (for details see Bignami et al., 1996; Jacchia et al., 1999). In the observations of Geminga at W.H. Keck Observatory the spectrum of a low resolution spanning 3700–8000Å with a broad dip over 6300–6400Å was obtained. But it is too noisy to give any definite conclusions on the spectral features in the optical emission of this pulsar.

The broad-band spectrum of the optical emission of another middle-aged neutron star, PSR B0656+14, reveals similar behavior (Koptsevich et al., 2001). This allows speaking about definite differencies in the emission of middle-aged INS if compared with that of younger and more energetic neutron stars like the Crab pulsar with the featureless spectra well described by a single power law with a spectral index

$\alpha_\nu \approx 0$ in a wide range from the IR to UV. Since the statistical errors of the estimates of faint fluxes of the neutron star optical emission existing so far are rather high, one needs further and deeper observations to confirm this hypothesis.

The paper presents the results of studies of the Geminga emission with the aid of the BVRI photometry from observations with the 6 m telescope of SAO RAS. The second chapter includes the description of observations, data reduction, photometric results and analysis of ISM properties toward this neutron star. The results and the features of the optical spectrum of Geminga are discussed in the third chapter. Their comparison with the observational data in the X- and EUV-rays shows an essentially non-thermal character of the Geminga emission in the red domain of the visible spectrum. Some ideas on further studies of objects of such a kind are considered.

2. Observations and data analysis

2.1. Observations and data reduction

Observations of the field of Geminga were carried out with the 6 m telescope in March, 1997, October, 1998 and January, 1999 with a CCD photometer mounted at the prime focus (Table 2). The set of filters close to the Johnson-Cousins system and CCD detectors

Table 3: *Technical specifications of CCD detectors*

Detector	Size (pixels)	Pixel size	FOV	Gain	Readout noise	η_{max}
ISD017A	1060×1170	$0''137$	$2'5 \times 3'0$	$2.3e^-/$ADU	$8e^-$	40%
Photometrics	1024×1024	$0''206$	$3'5 \times 3'5$	$1.3e^-/$ADU	$4e^-$	70%

Table 4: *Geminga coordinates at observational epochs*

Date	Calculated		Observed	
	α_{2000}	δ_{2000}	α_{2000}	δ_{2000}
1997.192	$06^h33^m54^s.18\pm0.01$	$17°46'12''.90\pm0.16$	$06^h33^m54^s.2\pm0.07$	$17°46'13''.5\pm0.9$
1998.803	$06^h33^m54^s.19\pm0.01$	$17°46'13''.06\pm0.16$	$06^h33^m54^s.3\pm0.07$	$17°46'14''.0\pm1.0$
1999.052	$06^h33^m54^s.20\pm0.01$	$17°46'13''.08\pm0.16$	$06^h33^m54^s.2\pm0.07$	$17°46'13''.8\pm0.8$

ISD017A (observations of 1997-1998) and Photometrics (observations of 1999) were used. Some of the characteristics of the detectors are given in Table 3. The range of spectral sensitivity for both detectors spans 3000–10000Å with a maximum in the red domain.

In March of 1997, 6 exposures in the R band and 8 in the B and V bands, each of 10 minutes duration, were taken. 21 images in the I band, exposure time being 5 minutes, were obtained in 1998. As a rule, the consequent exposures were shifted along one of the coordinates to simplify accounting of possible detector defects (e.g. "hot" pixels) and removing cosmic ray events. The atmosphere transparency and seeing varied during the observational night, so only part of the data was used in the analysis (Table 2). To check the photometric calibration additional individual images in the V, R and I bands were taken under good conditions in January, 1999. The secondary standard stars chosen are marked with an asterisk (*) in Table 5. See section 2.3 for more details.

The data were processed making use of the Munich Image Data Analysis System (MIDAS). Standard reduction, including bias subtraction, account for dark current, correction for non-uniformity of the detector sensitivity (flat-fielding), was performed with the aid of MIDAS context **ccdred**. Standard MIDAS procedures were used to remove cosmic ray events. We referred the individual images to a common coordinate frame to stack them together and to perform the world coordinate system astrometry.

2.2. Astrometric referencing

To define the Geminga coordinates at the observational epochs the data on the Geminga position on 1994.03 $\alpha_{1950} = 06^h30^m59^s.17$, $\delta_{1950} = 17°48'33''.82$ (Mignani et al., 1994) were used and its proper motion $\mu_\alpha = 138 \pm 4$ marcsec/year, $\mu_\delta = 97 \pm 4$ marcsec/year (Caraveo et al., 1996) was accounted for. The calculated and the observed coordinates of Geminga are given in Table 4.

To make the astrometric referencing, we used the coordinates of stars selected from the USNO-2 catalogue. The final accuracy of referencing to the world coordinate system is $1''$. Fig. 1 represents the field of the pulsar Geminga taken with the 6 m telescope in the R band. The stars are labelled in accordance with Table 5, where the photometry results are listed.

2.3. Photometry

Photometry of the field stars was done on the individual and combined BVRI images making use of the MIDAS context **daophot**. Besides, to the selected field objects, including Geminga, we applied the method of aperture photometry. As a rule, a set of 12 apertures was used, the radius of the minimum one being equal to HWHM and maximum – five times FWHM. The optimal aperture size was determined taking into account the signal-to-noise ratio (S/N) calculated as

$$\frac{S}{N} = f\left[\frac{f}{G} + A\,\sigma_f^2\left(1 + \frac{A}{A_{\text{sky}}}\right)\right]^{-1/2}, \quad (1)$$

where f – object flux in counts (DN) in the aperture chosen, σ_f – flux error (in DN), A – aperture size (in pixels), G – gain, A_{sky} – number of pixels used for background calculation.

Instrumental magnitudes in each filter m_j^{inst} were derived by the formula

$$m_j^{inst} = -2.5\log\left(\frac{f}{t_{\exp}}\right) - \frac{k}{\cos Z} - \delta m, \quad (2)$$

where f – object flux, k – extinction factor, Z – zenith distance, δm – correction for finite aperture, calculated from the point spread function (PSF) for the selected bright stars. The values of the extinction factors k averaged over the season, which are 0.25, 0.16, 0.11 and 0.06 for the B, V, R and I bands, respectively, were used.
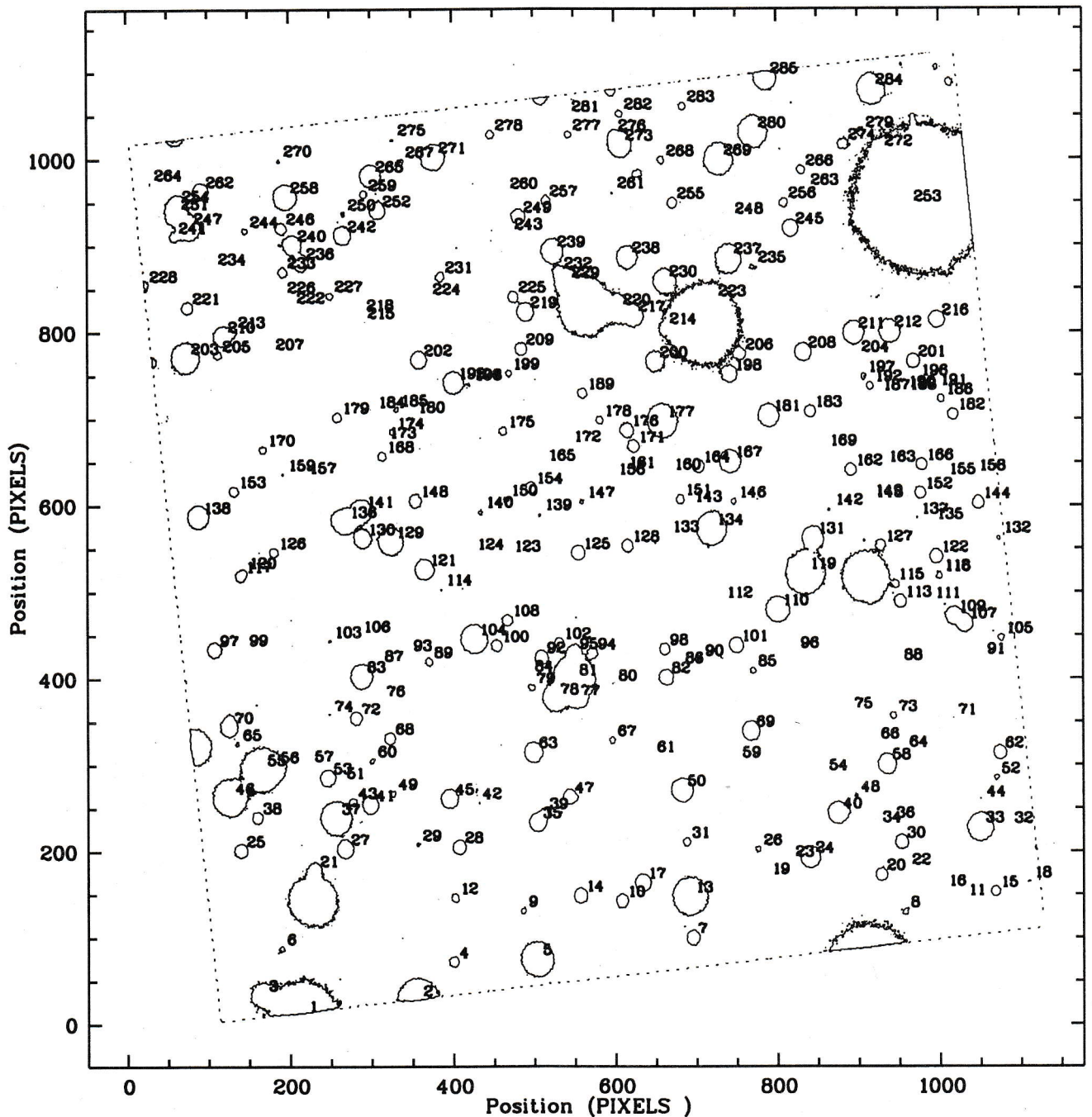
Figure 1: *Geminga pulsar (PSR J0633+1746) field as observed with the 6 m telescope. Numbers to label stars are the same as in Table 5 with the photometry results.*

To transfer instrumental magnitudes m_j^{inst} to those of the standard Johnson-Cousins system m_j^{st}, i.e. b, v, r and i to B, V, R and I, respectively, the photometric calibration was done making use of the observations of the Landolt standards PG1047, RU149, field SA92 and PG0918[1] (Landolt, 1992). To check the photometric calibration of the data obtained on

October 20, 1998, we used the results of photometry of the secondary field standard (marked by an asterisk in Table 5). This decreased the errors of the zero-point in photometric equations (6) to 0.02. The photometric equations (for each observational night in accordance with the dates in Table 2) are as follows:

---

[1] PG0918 was taken on October 20, 1998 under the conditions of changing transparency.

$$B = b + 0.13(0.02) \cdot (b - v) + 25.91(0.01)$$
$$V = v - 0.11(0.01) \cdot (b - v) + 26.26(0.02)$$
$$R = r + 0.02(0.01) \cdot (v - r) + 26.59(0.02) \tag{3}$$
$$I = i + 0.06(0.01) \cdot (r - i) + 25.7(0.04)$$

$$B = b + 0.13(0.03) \cdot (b - v) + 25.96(0.01)$$
$$V = v - 0.09(0.01) \cdot (b - v) + 26.27(0.01)$$
$$R = r + 26.59(0.02) \tag{4}$$
$$I = i + 0.11(0.03) \cdot (r - i) + 25.71(0.02)$$

$$B = b + 0.08(0.03) \cdot (b - v) + 26.16(0.03)$$
$$V = v - 0.11(0.03) \cdot (b - v) + 26.28(0.02)$$
$$R = r + 0.02(0.01) \cdot (v - r) + 26.59(0.02) \tag{5}$$
$$I = i + 0.06(0.02) \cdot (r - i) + 25.67(0.02)$$

$$R = r + 0.02(0.01) \cdot (v - r) + 26.59(0.02)$$
$$I = i + 0.06(0.02) \cdot (r - i) + 25.67(0.02) \tag{6}$$

$$B = b + 0.13(0.01) \cdot (b - v) + 26.47(0.01)$$
$$V = v - 0.10(0.05) \cdot (v - r) + 26.74(0.04)$$
$$R = r + 0.13(0.06) \cdot (v - r) + 27.22(0.04) \tag{7}$$
$$I = i + 0.14(0.01) \cdot (r - i) + 26.75(0.01)$$

$$B = b + 0.14(0.02) \cdot (b - v) + 26.59(0.01)$$
$$V = v - 0.10(0.01) \cdot (v - r) + 26.86(0.02)$$
$$R = r + 0.08(0.01) \cdot (v - r) + 27.35(0.02) \tag{8}$$
$$I = i + 0.13(0.04) \cdot (r - i) + 26.82(0.01)$$

The derived magnitudes of objects m_j^{st} were transformed to the absolute fluxes F_j (in erg$\cdot$ cm$^{-2}\cdot$ s$^{-1}\cdot$ Hz^{-1}) using the equation:

$$\log F_j = -(0.4 m_j^{st} + C_j^0) \tag{9}$$

with the zero-point C_j^0 provided by Fukugita et al. (1995).

$$C_B^0 = 19.396, \qquad C_V^0 = 19.445,$$
$$C_R^0 = 19.520, \qquad C_I^0 = 19.623. \tag{10}$$

2.4. Geminga and neighbouring objects

Fig. 2 represents the fragments of the Geminga field obtained with the 6 m telescope in the V, R and I bands of the Jonhson-Cousins system (with the total exposure time of 1800 s, 1800 s and 3900 s, respectively). The pulsar position is indicated with an arrow. The letters G and G′ stand for the objects, supposed to be the Geminga counterpart during the first optical observations of this field (Halpern & Tytler, 1988).
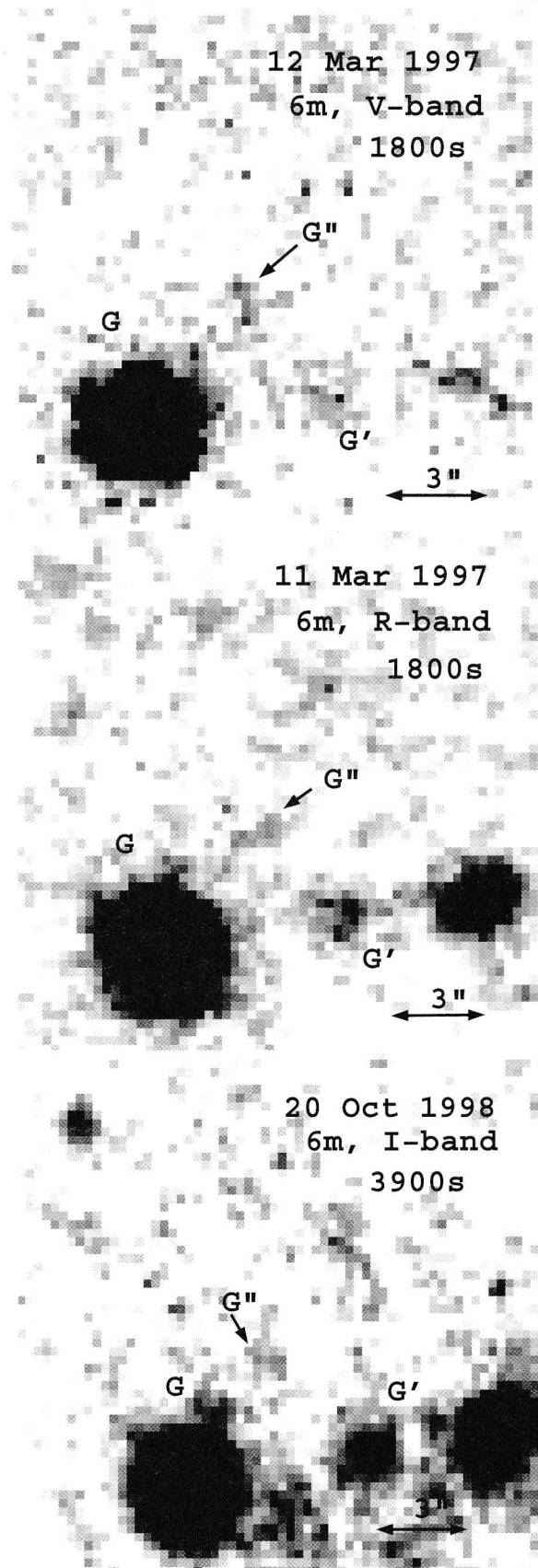

Figure 2: *Fragments of the images of the Geminga (G″) field as observed with 6 m telescope through the V, R and I filters.*

Table 5: BVR_cI_c-photometry of objects in the field of PSR J0633+1746

I	X	Y	V	B-V	V-R	R-I
1	217.20	11.74	14.10 ± 0.14	...	-0.73 ± 0.01	0.04 ± 0.02
2	357.43	29.06	15.92 ± 0.02	...	0.72 ± 0.02	0.70 ± 0.01
3	168.25	35.92	18.85 ± 0.01	...	0.58 ± 0.02	0.05 ± 0.02
4	401.73	73.60	21.98 ± 0.03	...	1.09 ± 0.03	1.05 ± 0.02
5	504.53	76.42	16.67 ± 0.01	...	0.50 ± 0.02	0.52 ± 0.01
6	190.71	89.08	23.21 ± 0.06	...	1.10 ± 0.03	0.93 ± 0.02
7	696.43	101.21	20.99 ± 0.02	...	0.99 ± 0.03	0.94 ± 0.02
8	958.48	131.21	22.82 ± 0.04	...	0.71 ± 0.02	0.70 ± 0.01
9	487.28	132.09	22.88 ± 0.04	...	1.10 ± 0.03	1.03 ± 0.02
10	609.22	143.88	21.13 ± 0.02	...	0.89 ± 0.03	0.80 ± 0.01
11	1029.22	145.14	24.27 ± 0.13	...	1.40 ± 0.04	1.86 ± 0.04
12	403.02	147.55	22.55 ± 0.03	...	1.23 ± 0.03	1.32 ± 0.03
13	693.28	148.79	17.18 ± 0.03	...	1.19 ± 0.03	0.40 ± 0.02
14	558.00	150.14	20.74 ± 0.02	...	0.93 ± 0.03	0.86 ± 0.02
15	1069.06	154.45	22.16 ± 0.03	...	1.23 ± 0.03	1.20 ± 0.02
16	1004.92	155.87	24.40 ± 0.14	...	1.04 ± 0.03	1.13 ± 0.02
17	634.64	165.06	19.92 ± 0.01	...	0.61 ± 0.02	0.63 ± 0.01
18	1110.46	165.34	23.31 ± 0.06	...	1.06 ± 0.03	1.11 ± 0.02
19	787.64	169.92	23.95 ± 0.10	...	1.20 ± 0.03	1.41 ± 0.03
20	929.22	174.04	21.23 ± 0.02	...	0.76 ± 0.03	0.72 ± 0.01
21	231.25	179.13	20.59 ± 0.02	...	0.69 ± 0.02	0.61 ± 0.01
22	960.14	180.45	24.57 ± 0.19	...	1.27 ± 0.04	1.40 ± 0.03
23	816.57	189.68	23.57 ± 0.08	...	1.07 ± 0.03	1.29 ± 0.02
24	841.28	194.42	19.18 ± 0.01	...	0.72 ± 0.02	0.72 ± 0.01
25	141.46	202.35	20.58 ± 0.01	...	0.59 ± 0.02	0.60 ± 0.01
26	777.60	203.21	23.34 ± 0.05	...	1.41 ± 0.04	1.27 ± 0.02
27	269.11	204.24	19.82 ± 0.01	...	0.66 ± 0.02	0.62 ± 0.01
28	408.85	206.33	20.57 ± 0.01	...	0.71 ± 0.02	0.66 ± 0.01
29	357.23	208.78	23.02 ± 0.05	...	1.01 ± 0.03	0.99 ± 0.02
30	953.94	211.68	20.81 ± 0.02	...	0.78 ± 0.03	0.78 ± 0.01
31	689.01	211.98	22.67 ± 0.04	...	1.23 ± 0.03	0.95 ± 0.02
32	1086.25	228.40	23.93 ± 0.09	...	0.79 ± 0.03	1.69 ± 0.04
33	1050.80	229.10	17.80 ± 0.01	...	0.70 ± 0.02	0.72 ± 0.01
34	924.18	229.73	24.18 ± 0.11	...	1.14 ± 0.03	1.37 ± 0.03
35	505.32	234.68	19.54 ± 0.01	...	0.60 ± 0.02	0.61 ± 0.01
36	940.90	234.72	24.14 ± 0.12	...	1.19 ± 0.03	1.16 ± 0.02
37	257.89	239.98	16.86 ± 0.01	...	0.49 ± 0.02	0.49 ± 0.01
38	161.65	240.77	21.43 ± 0.02	...	0.69 ± 0.02	0.62 ± 0.01
39	513.45	245.21	22.18 ± 0.03	...	0.94 ± 0.03	0.93 ± 0.02
40	875.36	245.54	19.15 ± 0.01	...	0.74 ± 0.03	0.72 ± 0.01
41	300.17	255.43	19.85 ± 0.01	...	0.68 ± 0.02	0.64 ± 0.01
			19.83 ± 0.01	1.33 ± 0.01	0.75 ± 0.02	...
42	430.77	257.33	22.84 ± 0.13	...	0.65 ± 0.02	1.20 ± 0.02
43	278.35	257.94	22.24 ± 0.04	...	0.78 ± 0.03	0.91 ± 0.02
44	1052.27	259.56	23.28 ± 0.06	...	0.99 ± 0.03	1.03 ± 0.02
45	397.09	262.34	19.68 ± 0.01	...	0.82 ± 0.03	0.81 ± 0.01
			19.67 ± 0.01	1.51 ± 0.01	0.89 ± 0.02	...
46	128.18	263.86	16.52 ± 0.01	...	0.47 ± 0.02	0.45 ± 0.02
47	544.65	264.17	20.51 ± 0.01	...	0.67 ± 0.02	0.74 ± 0.01
48	897.47	264.86	23.04 ± 0.04	...	0.78 ± 0.03	0.76 ± 0.01
49	327.54	268.51	22.93 ± 0.05	...	1.17 ± 0.03	1.27 ± 0.02
			22.83 ± 0.03	1.59 ± 0.01	1.20 ± 0.03	...
50	683.65	272.08	18.65 ± 0.01	...	0.70 ± 0.02	0.70 ± 0.01
51	264.18	281.54	25.34 ± 0.38	...	1.63 ± 0.04	1.50 ± 0.03

Table 5: BVR_cI_c-photometry of objects in the field of PSR J0633+1746 (continued)

I	X	Y	V	B-V	V-R	R-I
52	1070.48	285.88	23.13 ± 0.05	...	1.24 ± 0.03	1.23 ± 0.02
53	247.82	286.71	20.13 ± 0.01	...	0.66 ± 0.02	0.62 ± 0.01
54	858.27	290.05	24.07 ± 0.10	...	1.23 ± 0.03	1.35 ± 0.03
55	167.26	296.68	15.58 ± 0.01	...	0.25 ± 0.02	0.26 ± 0.02
56	183.32	299.84	18.98 ± 0.02	...	0.59 ± 0.02	0.78 ± 0.01
57	225.14	301.13	25.43 ± 0.36	...	1.62 ± 0.04	2.08 ± 0.05
58	936.33	302.21	19.27 ± 0.01	...	0.59 ± 0.02	0.64 ± 0.01
59	751.76	304.85	24.99 ± 0.23	...	1.34 ± 0.04	2.14 ± 0.05
60	302.70	306.31	22.91 ± 0.04	...	1.01 ± 0.03	1.00 ± 0.02
			22.94 ± 0.04	1.80 ± 0.01	1.16 ± 0.03	...
61	646.25	311.22	24.37 ± 0.14	...	1.34 ± 0.04	1.64 ± 0.03
			24.22 ± 0.10	1.51 ± 0.01	1.39 ± 0.03	...
62	1075.13	315.37	20.79 ± 0.02	...	0.84 ± 0.03	0.82 ± 0.02
63	500.65	315.63	19.39 ± 0.01	...	0.78 ± 0.03	0.73 ± 0.01
			19.37 ± 0.01	1.41 ± 0.01	0.84 ± 0.02	...
64	957.41	316.87	23.51 ± 0.07	...	1.09 ± 0.03	1.09 ± 0.02
65	137.50	325.95	22.99 ± 0.05	...	0.57 ± 0.02	0.34 ± 0.02
66	922.41	326.15	24.42 ± 0.15	...	1.50 ± 0.04	1.62 ± 0.03
			24.05 ± 0.09	1.31 ± 0.01	1.17 ± 0.03	...
67	597.76	329.66	23.47 ± 0.07	...	1.68 ± 0.04	1.83 ± 0.04
			23.21 ± 0.05	1.38 ± 0.01	1.52 ± 0.03	...
68*	324.24	332.29	21.03 ± 0.01	...	0.55 ± 0.02	0.55 ± 0.01
			21.02 ± 0.01	1.01 ± 0.01	0.59 ± 0.02	...
69	768.96	340.37	19.43 ± 0.01	...	0.62 ± 0.02	0.64 ± 0.01
			19.42 ± 0.01	1.09 ± 0.01	0.70 ± 0.02	...
70	127.58	345.69	19.74 ± 0.01	...	0.63 ± 0.02	0.62 ± 0.01
71	1017.91	354.06	23.42 ± 0.06	...	1.14 ± 0.03	1.01 ± 0.02
			23.41 ± 0.04	1.99 ± 0.01	1.19 ± 0.03	...
72	282.99	355.55	20.94 ± 0.01	...	0.71 ± 0.02	0.68 ± 0.01
73	944.55	357.91	23.02 ± 0.05	...	1.28 ± 0.04	1.54 ± 0.03
			22.92 ± 0.03	1.77 ± 0.01	1.33 ± 0.03	...
74	249.85	359.09	23.46 ± 0.06	...	1.15 ± 0.03	0.95 ± 0.02
75	889.71	361.39	24.19 ± 0.09	1.75 ± 0.01	1.22 ± 0.03	...
76	313.65	376.07	24.55 ± 0.13	1.48 ± 0.01	0.68 ± 0.02	...
77	552.95	376.33	21.44 ± 0.04	...	0.91 ± 0.03	1.10 ± 0.02
78	527.35	377.71	18.20 ± 0.01	...	0.55 ± 0.02	0.57 ± 0.01
			18.16 ± 0.01	0.99 ± 0.01	0.60 ± 0.02	...
79	498.11	390.05	23.01 ± 0.05	...	1.16 ± 0.03	0.97 ± 0.02
			22.92 ± 0.03	1.75 ± 0.01	1.14 ± 0.03	...
80	599.05	393.69	24.24 ± 0.14	...	1.73 ± 0.04	1.50 ± 0.03
81	550.73	399.94	15.64 ± 0.01	...	0.54 ± 0.02	0.48 ± 0.01
82	664.60	402.45	20.87 ± 0.02	...	1.15 ± 0.03	1.11 ± 0.02
			20.84 ± 0.01	1.90 ± 0.01	1.21 ± 0.03	...
83	289.96	404.02	18.48 ± 0.01	...	0.68 ± 0.02	0.61 ± 0.01
			18.45 ± 0.01	1.27 ± 0.01	0.74 ± 0.02	...
84	495.92	404.14	24.55 ± 0.13	2.40 ± 0.01	1.20 ± 0.03	...
85	771.53	410.16	23.12 ± 0.05	...	1.27 ± 0.04	1.14 ± 0.02
			23.08 ± 0.04	2.00 ± 0.01	1.34 ± 0.03	...
86	681.50	413.87	24.06 ± 0.10	...	1.00 ± 0.03	1.12 ± 0.02
			23.99 ± 0.07	2.02 ± 0.01	1.17 ± 0.03	...
87	311.34	416.63	24.24 ± 0.11	...	1.10 ± 0.03	1.60 ± 0.03
88	949.59	417.42	23.49 ± 0.08	...	1.21 ± 0.03	1.20 ± 0.02
			23.74 ± 0.07	1.92 ± 0.01	1.45 ± 0.03	...

Table 5: BVR_cI_c-photometry of objects in the field of PSR J0633+1746   (continued)

I	X	Y	V	B-V	V-R	R-I
89	372.05	420.48	22.46 ± 0.03	...	1.01 ± 0.03	0.85 ± 0.02
			22.29 ± 0.02	1.73 ± 0.01	0.94 ± 0.02	...
90	706.35	422.26	23.03 ± 0.04	...	0.96 ± 0.03	1.04 ± 0.02
			23.09 ± 0.03	2.21 ± 0.01	1.18 ± 0.03	...
91	1053.41	423.97	24.50 ± 0.15	...	1.21 ± 0.03	0.95 ± 0.02
92	510.85	425.19	21.25 ± 0.02	...	1.05 ± 0.03	0.94 ± 0.02
			21.16 ± 0.01	1.89 ± 0.01	1.08 ± 0.02	...
93	346.61	428.68	23.90 ± 0.09	...	1.19 ± 0.03	1.36 ± 0.03
94	573.66	430.04	22.49 ± 0.04	...	1.40 ± 0.04	1.60 ± 0.03
95	551.39	430.19	20.34 ± 0.01	...	0.60 ± 0.02	0.68 ± 0.01
			20.32 ± 0.01	0.99 ± 0.01	0.62 ± 0.02	...
94	573.21	430.98	22.36 ± 0.03	1.90 ± 0.01	1.38 ± 0.03	...
96	823.75	431.07	24.90 ± 0.21	...	1.13 ± 0.03	1.07 ± 0.02
97	109.72	434.69	20.62 ± 0.02	...	0.90 ± 0.03	0.78 ± 0.01
98	662.48	434.87	21.82 ± 0.02	...	1.13 ± 0.03	0.99 ± 0.02
			21.75 ± 0.02	1.82 ± 0.01	1.14 ± 0.03	...
99	145.68	435.31	24.78 ± 0.23	...	1.02 ± 0.03	1.05 ± 0.02
100	455.65	438.45	21.92 ± 0.02	...	1.09 ± 0.03	0.97 ± 0.02
			21.86 ± 0.02	1.79 ± 0.01	1.05 ± 0.02	...
101	751.22	439.23	20.36 ± 0.01	...	0.74 ± 0.03	0.75 ± 0.01
			20.31 ± 0.01	1.26 ± 0.01	0.78 ± 0.02	...
102	532.15	441.98	21.72 ± 0.02	...	0.56 ± 0.02	0.67 ± 0.01
			21.70 ± 0.01	0.94 ± 0.01	0.61 ± 0.02	...
103	249.93	444.35	23.29 ± 0.06	...	1.15 ± 0.03	1.27 ± 0.02
104	428.04	446.67	17.65 ± 0.01	...	0.56 ± 0.02	0.56 ± 0.01
			17.60 ± 0.01	1.04 ± 0.01	0.58 ± 0.02	...
105	1076.84	447.91	22.67 ± 0.03	...	1.00 ± 0.03	1.12 ± 0.02
106	285.50	450.70	24.26 ± 0.14	...	1.06 ± 0.03	0.98 ± 0.02
			24.07 ± 0.09	1.94 ± 0.01	1.18 ± 0.03	...
107	1032.11	464.96	20.02 ± 0.02	...	0.87 ± 0.03	0.79 ± 0.01
108*	468.58	468.24	21.47 ± 0.02	...	0.73 ± 0.03	0.68 ± 0.01
			21.44 ± 0.01	1.19 ± 0.01	0.77 ± 0.02	...
109	1018.64	473.28	19.91 ± 0.01	...	0.67 ± 0.02	0.66 ± 0.01
			19.89 ± 0.01	1.22 ± 0.01	0.68 ± 0.02	...
110	801.97	480.50	18.31 ± 0.01	...	0.58 ± 0.02	0.59 ± 0.01
			18.30 ± 0.01	0.99 ± 0.01	0.66 ± 0.02	...
111	989.63	488.53	25.33 ± 0.33	0.53 ± 0.01	1.64 ± 0.03	...
112	732.89	489.34	24.48 ± 0.16	...	0.96 ± 0.03	1.75 ± 0.04
			24.46 ± 0.11	1.77 ± 0.01	1.21 ± 0.03	...
113	953.30	489.89	21.39 ± 0.02	...	0.92 ± 0.03	0.86 ± 0.02
			21.36 ± 0.01	1.48 ± 0.01	0.94 ± 0.02	...
114	387.34	504.74	23.05 ± 0.04	...	0.72 ± 0.03	0.69 ± 0.01
			22.84 ± 0.03	1.28 ± 0.01	0.68 ± 0.02	...
115	944.30	510.31	23.07 ± 0.07	...	1.14 ± 0.03	1.24 ± 0.02
			22.91 ± 0.04	1.63 ± 0.01	1.02 ± 0.02	...
116	1001.51	519.62	22.75 ± 0.04	...	0.98 ± 0.03	0.91 ± 0.02
117	141.73	519.92	21.47 ± 0.02	...	0.53 ± 0.02	0.62 ± 0.01
118	1001.00	520.43	22.70 ± 0.03	1.42 ± 0.01	0.93 ± 0.02	...
119	835.80	522.58	16.12 ± 0.01	...	0.55 ± 0.02	0.57 ± 0.01
120	145.97	524.68	23.20 ± 0.15	...	1.37 ± 0.04	0.72 ± 0.01
121	366.99	527.38	19.06 ± 0.01	...	0.55 ± 0.02	0.58 ± 0.01
			19.02 ± 0.01	0.96 ± 0.01	0.59 ± 0.02	...
122*	997.42	541.73	20.82 ± 0.01	...	0.72 ± 0.02	0.71 ± 0.01

Table 5: BVR_cI_c-photometry of objects in the field of PSR J0633+1746 (continued)

I	X	Y	V	B-V	V-R	R-I
			20.79 ± 0.01	1.32 ± 0.01	0.74 ± 0.02	...
123	470.53	542.83	23.96 ± 0.09	...	1.29 ± 0.04	1.15 ± 0.02
			23.83 ± 0.07	1.59 ± 0.01	1.35 ± 0.03	...
124	425.12	545.38	24.90 ± 0.22	...	1.09 ± 0.03	1.50 ± 0.03
			24.97 ± 0.21	0.80 ± 0.01	1.16 ± 0.03	...
125	556.21	545.86	20.57 ± 0.01	...	0.68 ± 0.02	0.65 ± 0.01
			20.51 ± 0.01	1.21 ± 0.01	0.71 ± 0.02	...
126	182.31	547.16	22.05 ± 0.03	...	0.98 ± 0.03	0.84 ± 0.02
127	928.98	554.17	22.18 ± 0.03	...	0.93 ± 0.03	0.91 ± 0.02
			22.12 ± 0.02	1.33 ± 0.01	1.02 ± 0.02	...
128*	616.93	554.30	21.03 ± 0.01	...	0.58 ± 0.02	0.58 ± 0.01
			20.99 ± 0.01	1.00 ± 0.01	0.61 ± 0.02	...
129	326.33	559.51	17.95 ± 0.01	...	0.53 ± 0.02	0.55 ± 0.01
			17.92 ± 0.01	0.92 ± 0.01	0.59 ± 0.02	...
130	291.67	562.80	19.90 ± 0.01	...	0.69 ± 0.02	0.70 ± 0.01
			19.88 ± 0.01	1.22 ± 0.01	0.75 ± 0.02	...
131	845.77	563.31	19.04 ± 0.01	...	0.76 ± 0.03	0.74 ± 0.01
			18.99 ± 0.01	1.34 ± 0.01	0.81 ± 0.02	...
132	1074.28	563.91	23.34 ± 0.06	...	1.15 ± 0.03	1.14 ± 0.02
133	666.11	565.63	24.95 ± 0.25	...	1.98 ± 0.05	1.22 ± 0.02
			24.56 ± 0.15	1.32 ± 0.01	1.58 ± 0.03	...
134	721.03	573.65	17.25 ± 0.01	...	0.64 ± 0.02	0.60 ± 0.01
			17.22 ± 0.01	1.21 ± 0.01	0.68 ± 0.02	...
135	991.63	579.72	24.92 ± 0.20	...	0.98 ± 0.03	0.87 ± 0.02
136	269.20	582.94	18.29 ± 0.01	...	0.57 ± 0.02	0.58 ± 0.01
			18.26 ± 0.01	1.01 ± 0.01	0.61 ± 0.02	...
137	972.88	585.91	23.92 ± 0.08	...	1.03 ± 0.03	1.35 ± 0.03
138	90.01	588.29	18.73 ± 0.01	...	0.69 ± 0.02	0.64 ± 0.01
139	508.71	590.72	24.48 ± 0.17	...	1.98 ± 0.05	1.91 ± 0.04
			23.93 ± 0.09	1.67 ± 0.01	1.55 ± 0.03	...
140	435.90	593.89	23.15 ± 0.05	...	1.06 ± 0.03	0.97 ± 0.02
			23.28 ± 0.05	1.71 ± 0.01	1.27 ± 0.03	...
141	289.80	594.95	18.66 ± 0.01	...	0.60 ± 0.02	0.60 ± 0.01
			18.65 ± 0.01	1.10 ± 0.01	0.66 ± 0.02	...
142	867.14	596.57	24.19 ± 0.11	...	1.45 ± 0.04	0.95 ± 0.02
			23.96 ± 0.09	1.56 ± 0.01	1.45 ± 0.03	...
143	693.97	600.41	24.98 ± 0.25	...	1.48 ± 0.04	1.62 ± 0.03
144	1049.21	604.11	21.36 ± 0.02	...	0.99 ± 0.03	0.94 ± 0.02
145	916.92	605.16	24.56 ± 0.16	...	1.55 ± 0.04	1.47 ± 0.03
146	748.38	605.35	23.24 ± 0.06	...	1.16 ± 0.03	1.45 ± 0.03
			23.19 ± 0.05	1.96 ± 0.01	1.27 ± 0.03	...
147	561.23	605.45	23.75 ± 0.09	...	1.51 ± 0.04	1.60 ± 0.03
			23.52 ± 0.06	2.11 ± 0.01	1.45 ± 0.03	...
148*	356.01	606.70	21.96 ± 0.03	...	1.14 ± 0.03	1.06 ± 0.02
			21.99 ± 0.03	2.20 ± 0.01	1.18 ± 0.03	...
149	916.32	607.27	24.12 ± 0.10	2.55 ± 0.01	1.38 ± 0.03	...
150	466.71	607.45	23.38 ± 0.06	...	1.28 ± 0.04	1.24 ± 0.02
			23.46 ± 0.06	1.45 ± 0.01	1.47 ± 0.03	...
151	682.00	608.23	22.74 ± 0.04	...	1.27 ± 0.04	1.46 ± 0.03
			22.70 ± 0.03	2.02 ± 0.01	1.38 ± 0.03	...
152	978.06	615.33	21.42 ± 0.02	...	0.83 ± 0.03	0.81 ± 0.01
			21.43 ± 0.01	1.43 ± 0.01	0.91 ± 0.02	...
153	133.39	618.13	22.14 ± 0.03	...	1.18 ± 0.03	1.18 ± 0.02

Table 5: BVR_cI_c-photometry of objects in the field of PSR J0633+1746 (continued)

I	X	Y	V	B-V	V-R	R-I
154	498.15	621.42	22.25 ± 0.03	...	1.42 ± 0.04	1.52 ± 0.03
			22.11 ± 0.02	1.95 ± 0.01	1.38 ± 0.03	...
155	1006.82	631.91	23.74 ± 0.08	...	1.08 ± 0.03	1.17 ± 0.02
			23.84 ± 0.26	2.59 ± 0.01	1.33 ± 0.03	...
156	599.53	632.03	24.63 ± 0.17	...	1.45 ± 0.04	1.30 ± 0.02
			24.42 ± 0.15	1.79 ± 0.01	1.59 ± 0.03	...
157	219.33	634.25	24.33 ± 0.13	...	1.18 ± 0.03	1.32 ± 0.03
158	1043.73	635.98	23.77 ± 0.09	...	1.23 ± 0.03	1.31 ± 0.03
159	193.58	637.39	23.18 ± 0.05	...	0.98 ± 0.03	1.06 ± 0.02
160	668.48	637.76	24.30 ± 0.12	...	1.10 ± 0.03	1.13 ± 0.02
			24.12 ± 0.08	1.74 ± 0.01	1.02 ± 0.02	...
161	612.23	639.92	24.10 ± 0.11	...	1.42 ± 0.04	1.52 ± 0.03
			24.13 ± 0.10	1.20 ± 0.01	1.58 ± 0.03	...
162	892.18	642.23	21.74 ± 0.02	...	1.20 ± 0.03	1.09 ± 0.02
			21.67 ± 0.02	1.79 ± 0.01	1.25 ± 0.03	...
163	931.95	645.60	24.35 ± 0.10	0.14 ± 0.01	0.65 ± 0.02	...
			24.78 ± 0.20	...	0.91 ± 0.03	1.01 ± 0.02
164	704.63	646.25	21.74 ± 0.03	...	1.34 ± 0.04	1.54 ± 0.03
			21.65 ± 0.02	1.80 ± 0.01	1.32 ± 0.03	...
165	513.61	647.89	24.64 ± 0.17	...	1.37 ± 0.04	1.42 ± 0.03
166	979.54	648.26	21.61 ± 0.02	...	1.02 ± 0.03	0.94 ± 0.02
			21.59 ± 0.02	1.66 ± 0.01	1.10 ± 0.03	...
167	743.97	651.78	18.79 ± 0.01	...	0.63 ± 0.02	0.61 ± 0.01
			18.76 ± 0.01	1.13 ± 0.01	0.68 ± 0.02	...
168	314.78	658.22	22.48 ± 0.03	...	1.17 ± 0.03	1.06 ± 0.02
			22.38 ± 0.02	1.85 ± 0.01	1.20 ± 0.03	...
169	860.31	665.20	24.40 ± 0.13	...	1.32 ± 0.04	1.62 ± 0.03
			24.45 ± 0.11	1.74 ± 0.01	1.44 ± 0.03	...
170	168.88	666.20	22.71 ± 0.04	...	1.23 ± 0.03	1.33 ± 0.03
171	624.52	669.26	21.80 ± 0.02	...	1.12 ± 0.03	0.95 ± 0.02
			21.69 ± 0.02	1.74 ± 0.01	1.14 ± 0.03	...
172	544.64	669.78	25.06 ± 0.26	...	1.51 ± 0.04	1.42 ± 0.03
			24.59 ± 0.15	1.76 ± 0.01	1.10 ± 0.03	...
173	317.63	674.76	24.46 ± 0.16	...	1.48 ± 0.04	1.28 ± 0.02
			24.13 ± 0.10	1.88 ± 0.01	1.26 ± 0.03	...
174	327.48	685.59	22.75 ± 0.04	...	1.03 ± 0.03	0.96 ± 0.02
			22.68 ± 0.03	1.53 ± 0.01	1.08 ± 0.02	...
175*	463.46	686.62	22.31 ± 0.02	...	0.78 ± 0.03	0.84 ± 0.02
			22.33 ± 0.02	1.27 ± 0.01	0.75 ± 0.02	...
176	616.22	687.91	20.67 ± 0.01	...	0.60 ± 0.02	0.69 ± 0.01
			20.62 ± 0.01	1.05 ± 0.01	0.64 ± 0.02	...
177	660.20	698.53	17.27 ± 0.01	...	0.63 ± 0.02	0.62 ± 0.01
			17.24 ± 0.01	1.09 ± 0.01	0.66 ± 0.02	...
178	582.54	699.32	22.64 ± 0.03	...	1.01 ± 0.03	1.04 ± 0.02
			22.61 ± 0.02	1.82 ± 0.01	1.08 ± 0.02	...
179	259.95	703.29	21.75 ± 0.02	...	0.64 ± 0.02	0.72 ± 0.01
			21.79 ± 0.01	1.24 ± 0.01	0.77 ± 0.02	...
180	352.81	703.98	24.65 ± 0.19	...	2.11 ± 0.05	1.62 ± 0.03
			24.14 ± 0.10	1.93 ± 0.01	1.75 ± 0.04	...
181	791.64	704.88	18.69 ± 0.01	...	0.52 ± 0.02	0.53 ± 0.01
			18.65 ± 0.01	0.90 ± 0.01	0.56 ± 0.02	...
182	1018.16	706.47	21.88 ± 0.02	...	1.19 ± 0.03	1.18 ± 0.02
183	842.27	709.64	21.79 ± 0.02	...	1.20 ± 0.03	1.22 ± 0.02

Table 5: BVR_cI_c-photometry of objects in the field of PSR J0633+1746 (continued)

I	X	Y	V	B-V	V-R	R-I
			21.72 ± 0.02	1.82 ± 0.01	1.26 ± 0.03	...
184	303.99	710.08	25.13 ± 0.28	...	1.73 ± 0.04	1.32 ± 0.03
			24.38 ± 0.13	1.38 ± 0.01	1.16 ± 0.03	...
185	331.99	711.62	23.32 ± 0.06	...	1.25 ± 0.03	1.23 ± 0.02
			23.27 ± 0.04	1.68 ± 0.01	1.34 ± 0.03	...
186	1003.62	723.86	23.09 ± 0.05	...	1.48 ± 0.04	1.70 ± 0.04
187	925.99	728.98	24.97 ± 0.20	...	0.18 ± 0.02	1.93 ± 0.04
188	958.80	729.45	24.26 ± 0.12	...	1.17 ± 0.03	1.41 ± 0.03
189	561.56	730.30	22.19 ± 0.02	...	1.05 ± 0.03	0.93 ± 0.02
			22.18 ± 0.02	1.64 ± 0.01	1.13 ± 0.03	...
190	957.61	732.45	24.52 ± 0.15	1.34 ± 0.01	1.51 ± 0.03	...
191	996.70	734.53	24.93 ± 0.22	...	0.81 ± 0.03	1.43 ± 0.03
192	916.42	739.01	22.47 ± 0.03	...	0.91 ± 0.03	0.74 ± 0.01
			22.53 ± 0.02	1.16 ± 0.01	1.02 ± 0.02	...
193	422.91	741.17	23.56 ± 0.06	0.55 ± 0.01	0.88 ± 0.02	...
194	421.38	741.98	23.34 ± 0.06	...	0.87 ± 0.03	0.64 ± 0.01
195	402.60	742.65	18.90 ± 0.01	...	0.55 ± 0.02	0.58 ± 0.01
			18.87 ± 0.01	0.93 ± 0.01	0.61 ± 0.02	...
196	972.97	745.48	24.46 ± 0.14	...	0.76 ± 0.03	1.41 ± 0.03
197	907.77	749.77	22.91 ± 0.04	...	0.95 ± 0.03	0.89 ± 0.02
			22.94 ± 0.04	1.46 ± 0.01	0.92 ± 0.02	...
198	743.81	751.92	20.89 ± 0.02	...	0.86 ± 0.03	0.83 ± 0.02
			20.88 ± 0.01	1.44 ± 0.01	0.92 ± 0.02	...
199	469.42	753.23	23.21 ± 0.05	...	1.31 ± 0.04	1.28 ± 0.02
			23.05 ± 0.04	2.17 ± 0.01	1.31 ± 0.03	...
200	651.14	766.68	19.67 ± 0.01	...	0.61 ± 0.02	0.63 ± 0.01
			19.63 ± 0.01	1.06 ± 0.01	0.65 ± 0.02	...
201	969.66	767.18	21.16 ± 0.02	...	1.12 ± 0.03	1.11 ± 0.02
			21.19 ± 0.02	2.03 ± 0.01	1.24 ± 0.03	...
202*	360.42	769.12	19.87 ± 0.01	...	0.55 ± 0.02	0.59 ± 0.01
			19.85 ± 0.01	0.91 ± 0.01	0.59 ± 0.02	...
203	74.80	772.07	17.18 ± 0.01	...	0.33 ± 0.02	0.37 ± 0.02
204	899.79	772.63	24.44 ± 0.13	...	1.10 ± 0.03	1.38 ± 0.03
			24.71 ± 0.18	0.79 ± 0.01	1.66 ± 0.03	...
205	113.64	774.80	22.60 ± 0.04	...	1.09 ± 0.03	1.23 ± 0.02
206	756.97	775.38	22.19 ± 0.03	...	0.87 ± 0.03	1.07 ± 0.02
			22.06 ± 0.02	1.42 ± 0.01	0.86 ± 0.02	...
207	178.81	777.02	24.19 ± 0.12	...	1.26 ± 0.03	1.45 ± 0.03
208	834.00	777.43	20.20 ± 0.02	...	1.02 ± 0.03	0.94 ± 0.02
			20.18 ± 0.01	1.67 ± 0.01	1.09 ± 0.02	...
209	486.10	781.12	21.23 ± 0.02	...	0.72 ± 0.03	0.73 ± 0.01
			21.24 ± 0.01	1.22 ± 0.01	0.83 ± 0.02	...
210	120.43	796.94	19.63 ± 0.02	...	0.82 ± 0.03	0.77 ± 0.01
211	895.92	799.64	18.85 ± 0.01	...	0.65 ± 0.02	0.60 ± 0.01
			18.82 ± 0.01	1.13 ± 0.01	0.70 ± 0.02	...
212	940.58	801.15	18.73 ± 0.01	...	0.54 ± 0.02	0.52 ± 0.01
			18.72 ± 0.01	0.93 ± 0.01	0.62 ± 0.02	...
213	132.89	802.54	22.19 ± 0.03	...	0.92 ± 0.03	0.78 ± 0.01
214	663.29	805.32	21.94 ± 0.02	1.19 ± 0.01	0.76 ± 0.02	...
215	291.80	813.50	23.31 ± 0.06	...	0.94 ± 0.03	0.87 ± 0.02
			23.39 ± 0.06	1.19 ± 0.01	0.74 ± 0.02	...
216	998.72	814.83	20.15 ± 0.01	...	0.63 ± 0.02	0.65 ± 0.01
217	624.63	819.65	19.37 ± 0.01	...	0.57 ± 0.02	0.57 ± 0.01

Table 5: BVR_cI_c-photometry of objects in the field of PSR J0633+1746   (continued)

I	X	Y	V	B-V	V-R	R-I
			19.35 ± 0.01	1.00 ± 0.01	0.63 ± 0.02	...
218	290.36	821.74	24.21 ± 0.10	0.53 ± 0.01	1.15 ± 0.03	...
219	491.39	823.76	19.87 ± 0.01	...	0.67 ± 0.02	0.67 ± 0.01
			19.85 ± 0.01	1.17 ± 0.01	0.72 ± 0.02	...
220	605.68	827.28	18.30 ± 0.01	...	0.47 ± 0.02	0.50 ± 0.01
			18.28 ± 0.01	0.80 ± 0.01	0.52 ± 0.02	...
221	76.80	830.06	21.29 ± 0.02	...	0.82 ± 0.03	0.87 ± 0.02
222	204.60	830.48	23.98 ± 0.10	...	1.04 ± 0.03	0.95 ± 0.02
223	723.71	837.06	18.44 ± 0.01	...	0.58 ± 0.02	0.67 ± 0.01
			18.43 ± 0.01	0.93 ± 0.01	0.61 ± 0.02	...
224	371.27	839.90	24.80 ± 0.20	...	1.29 ± 0.04	1.86 ± 0.04
			24.80 ± 0.18	1.62 ± 0.01	1.24 ± 0.03	...
225	476.63	841.40	21.99 ± 0.02	...	1.00 ± 0.03	0.93 ± 0.02
			21.98 ± 0.02	1.66 ± 0.01	1.10 ± 0.03	...
226	193.24	842.57	24.35 ± 0.21	...	1.26 ± 0.03	1.43 ± 0.03
227	251.25	843.59	22.45 ± 0.03	...	0.86 ± 0.03	0.78 ± 0.01
			22.43 ± 0.03	1.40 ± 0.01	0.96 ± 0.02	...
228	23.40	855.62	22.75 ± 0.05	...	1.35 ± 0.04	1.28 ± 0.02
229	542.49	858.12	18.62 ± 0.01	...	0.58 ± 0.02	0.59 ± 0.01
			18.60 ± 0.01	0.96 ± 0.01	0.63 ± 0.02	...
230	663.12	859.67	18.87 ± 0.01	...	0.60 ± 0.02	0.60 ± 0.01
			18.85 ± 0.01	1.08 ± 0.01	0.66 ± 0.02	...
231*	386.40	864.79	22.29 ± 0.03	...	1.06 ± 0.03	0.83 ± 0.02
			22.29 ± 0.02	1.55 ± 0.01	1.10 ± 0.03	...
232	533.23	868.97	22.31 ± 0.03	...	0.97 ± 0.03	0.98 ± 0.02
			22.04 ± 0.02	1.29 ± 0.01	0.89 ± 0.02	...
233	193.35	870.88	22.37 ± 0.03	...	1.26 ± 0.03	1.34 ± 0.03
234	108.36	875.55	24.19 ± 0.14	...	1.16 ± 0.03	1.34 ± 0.03
235	772.79	875.64	23.75 ± 0.09	...	1.48 ± 0.04	1.25 ± 0.02
			23.78 ± 0.09	2.41 ± 0.01	1.27 ± 0.03	...
236	216.32	881.23	20.20 ± 0.01	...	0.73 ± 0.03	0.72 ± 0.01
237	742.84	885.47	18.12 ± 0.01	...	0.58 ± 0.02	0.57 ± 0.01
			18.09 ± 0.01	1.02 ± 0.01	0.64 ± 0.02	...
238	617.23	886.82	18.95 ± 0.01	...	0.55 ± 0.02	0.56 ± 0.01
			18.94 ± 0.01	0.94 ± 0.01	0.59 ± 0.02	...
239	524.93	893.67	18.57 ± 0.01	...	0.55 ± 0.02	0.54 ± 0.01
			18.56 ± 0.01	0.91 ± 0.01	0.61 ± 0.02	...
240	205.80	901.88	19.94 ± 0.02	...	1.13 ± 0.03	1.35 ± 0.03
241	59.95	911.55	22.24 ± 0.03	...	0.96 ± 0.03	1.02 ± 0.02
242	267.02	912.46	20.07 ± 0.02	...	0.97 ± 0.03	0.88 ± 0.02
243	471.97	914.11	23.56 ± 0.07	...	0.98 ± 0.03	1.04 ± 0.02
			23.94 ± 0.09	1.12 ± 0.01	1.47 ± 0.03	...
244	147.73	918.34	23.15 ± 0.06	...	1.35 ± 0.04	1.52 ± 0.03
245	818.93	920.08	20.29 ± 0.02	...	0.87 ± 0.03	0.73 ± 0.01
			20.27 ± 0.01	1.49 ± 0.01	0.94 ± 0.02	...
246	191.93	921.32	21.94 ± 0.03	...	1.22 ± 0.03	1.28 ± 0.02
247	78.55	922.36	18.13 ± 0.01	...	0.61 ± 0.02	0.61 ± 0.01
248	744.54	931.88	23.82 ± 0.09	...	1.13 ± 0.03	1.43 ± 0.03
			23.95 ± 0.12	1.79 ± 0.01	1.40 ± 0.03	...
249	483.11	933.40	20.49 ± 0.01	...	0.73 ± 0.03	0.75 ± 0.01
250	267.55	937.27	23.60 ± 0.08	...	1.46 ± 0.04	0.93 ± 0.02
251	63.03	939.17	18.59 ± 0.01	...	0.58 ± 0.02	0.60 ± 0.01
252	310.22	941.28	20.19 ± 0.02	...	0.82 ± 0.03	0.76 ± 0.01

Table 5: BVR_cI_c-photometry of objects in the field of PSR J0633+1746   (continued)

I	X°	Y°	V	B−V	V−R	R−I
253	964.49	945.59	18.22 ± 0.08	0.04 ± 0.01	0.68 ± 0.02	...
254	64.16	948.13	19.39 ± 0.01	...	0.67 ± 0.02	0.67 ± 0.01
255*	672.79	949.60	22.03 ± 0.02	...	1.07 ± 0.03	0.91 ± 0.02
			22.02 ± 0.02	1.75 ± 0.01	1.18 ± 0.03	...
256	810.31	949.73	21.99 ± 0.02	...	0.67 ± 0.02	0.50 ± 0.01
			21.98 ± 0.02	1.11 ± 0.01	0.68 ± 0.02	...
257	515.61	952.05	22.78 ± 0.07	...	1.35 ± 0.04	0.71 ± 0.01
258	197.41	957.45	18.03 ± 0.01	...	0.48 ± 0.02	0.49 ± 0.01
259	292.96	959.89	22.61 ± 0.03	...	0.98 ± 0.03	0.91 ± 0.02
260	466.86	961.04	24.31 ± 0.13	...	1.32 ± 0.04	0.72 ± 0.01
261	599.33	961.69	23.58 ± 0.07	...	1.05 ± 0.03	1.07 ± 0.02
262	93.62	964.22	19.85 ± 0.01	...	0.59 ± 0.02	0.63 ± 0.01
263	837.96	964.96	24.02 ± 0.10	...	1.08 ± 0.03	1.45 ± 0.03
			23.79 ± 0.11	1.36 ± 0.01	1.28 ± 0.03	...
264	29.74	972.70	23.64 ± 0.08	...	1.08 ± 0.03	0.86 ± 0.02
265	301.75	981.30	18.67 ± 0.01	...	0.52 ± 0.02	0.57 ± 0.01
266	831.57	987.21	22.64 ± 0.04	...	1.11 ± 0.03	1.13 ± 0.02
267	338.56	997.83	23.69 ± 0.09	...	1.76 ± 0.04	1.77 ± 0.04
268	659.56	998.86	22.76 ± 0.04	...	1.14 ± 0.03	0.90 ± 0.02
269	730.78	999.56	17.32 ± 0.01	...	0.56 ± 0.02	0.52 ± 0.01
270	189.18	999.81	22.66 ± 0.03	...	0.63 ± 0.02	0.53 ± 0.01
271	378.85	1002.53	18.10 ± 0.01	...	0.55 ± 0.02	0.57 ± 0.01
272	929.09	1009.82	21.34 ± 0.02	...	0.55 ± 0.02	1.06 ± 0.02
273	609.01	1016.69	18.20 ± 0.01	...	0.57 ± 0.02	0.55 ± 0.01
274	883.90	1017.27	22.87 ± 0.05	...	1.21 ± 0.03	0.88 ± 0.02
275	329.04	1023.54	24.30 ± 0.15	...	1.86 ± 0.05	1.91 ± 0.04
276	600.66	1028.22	22.16 ± 0.03	...	0.75 ± 0.03	1.16 ± 0.02
277	544.42	1028.31	22.76 ± 0.04	...	1.12 ± 0.03	1.18 ± 0.02
278	448.32	1028.44	21.92 ± 0.02	...	0.68 ± 0.02	0.54 ± 0.01
279	905.77	1031.16	23.51 ± 0.07	...	1.23 ± 0.03	1.38 ± 0.03
280	773.08	1031.25	17.25 ± 0.01	...	0.50 ± 0.02	0.48 ± 0.01
281	543.28	1050.07	24.88 ± 0.29	...	1.92 ± 0.05	1.38 ± 0.03
282	607.90	1052.89	22.76 ± 0.04	...	1.05 ± 0.03	0.99 ± 0.02
283	685.60	1061.55	22.80 ± 0.04	...	1.20 ± 0.03	1.21 ± 0.02
284	918.11	1080.75	17.59 ± 0.01	...	0.56 ± 0.02	0.53 ± 0.01
285	788.34	1093.91	18.44 ± 0.01	...	0.61 ± 0.02	0.60 ± 0.01

An analysis of individual images in the R and I bands obtained on January 19, 1999 with an arc-second seeing revealed the object G to be a double one. Then it became evident that G′ is extended. This supposition arose earlier when we compared the Geminga field images obtained with the 6 m telescope in the V band with the *HST* ones, taken in the F555W filter (Bignami et al., 1996). G′ is likely to be a background galaxy.

Geminga (G″) is evidently detected in the combined images in the V, R and I bands. As for the B band, the poor sensitivity of CCD detector ISD017A in this domain and insufficient total exposure time with the best seeing (1″6) provided the detection of the object at a level of S/N = 2.5 only. Nevertheless, we decided not to discard these data from consideration but performed photometry, the center of the aperture being placed in accordance with the Geminga position in the V band image.

The BVRI photometry yielded estimates of the magnitudes and fluxes of the pulsar emission and also those for the field objects mentioned [2] (Table 6). Our results are in good agreement with those of other observations, the I magnitude being an exception. Our estimate, $25{\overset{m}{.}}1\pm0.4$, is significantly different from the upper limit ($26{\overset{m}{.}}4$) given by Bignami et al. (1996). It should be noted that in their paper the limit was set to be of $25{\overset{m}{.}}4$ magnitude. Meanwhile, the flux estimate ($\sim 0.6 \times 10^{-30}$ erg/cm²s Hz) shown in Figure 4 of that paper does not correspond to the value reported. In the paper of the same authors appeared a few years later, which compiled all the data on the Geminga I–optical–UV emission obtained with CFHT, NTT, 3.6 m ESO and *HST*, the value of $26{\overset{m}{.}}4$ and the corresponding flux estimate were quoted in

---

[2] The integral values are given for the object G, as it is unresolved in the B and V images.

Table 6: *BVRI-photometry of PSR J0633+1746 (G″ or Geminga) and neighbouring objects*

	B		V		R		I	
	Magnitude	Flux*	Magnitude	Flux*	Magnitude	Flux*	Magnitude	Flux*
G	22.1	58.1	21.0±0.1	143	20.4±0.1	209	19.8±0.2	286
G′	>26.1	<1.58	24.5±0.3	5.68	24.3±0.3	5.75	23.5±0.4	9.48
G″	26.1±0.5	1.46	25.3±0.3	2.72	25.4±0.3	2.09	25.1±0.4	2.17

* − 10^{-30} erg/(cm² s Hz)
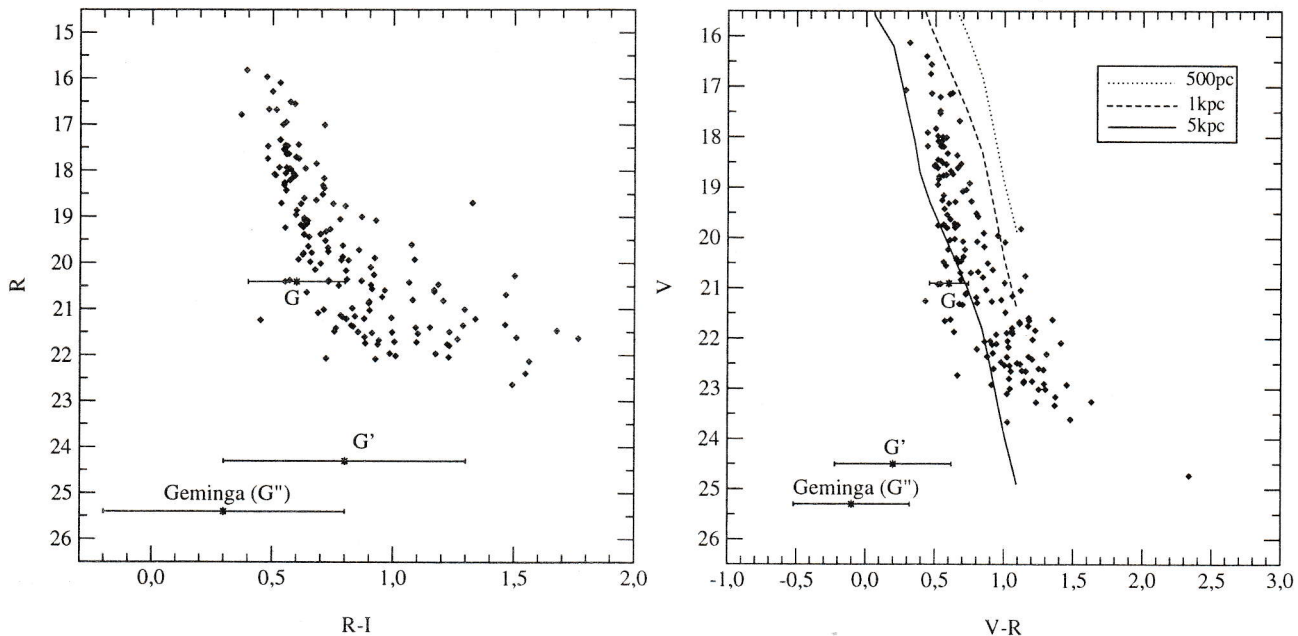
Figure 3: *"Colour-magnitude" diagrams for Geminga and field objects (Table 6 and Table 5). The errors are 0.02 mag for the brightest stars and up to 0.4 near the level of detection. Lines correspond to the colour-magnitude dependence for unreddened main sequence stars at distances of 0.5, 1 and 5 kpc.*

accordance with the figure previously discussed.

2.5. Field objects and properties of ISM toward Geminga

Geminga is very close to the Galaxy plane (height $z = 12$ pc), so its emission may be reddened. Upper limits of interstellar extinction in our Galaxy toward Geminga (l=195.134, b=4.265), estimated making use of the maps of infrared radiation of dust from the paper of Schlegel et al. (1998) (the programme of O. Verkhodanov was used), are $A_V \sim 1.7$, $E(B-V) = 0.54$, $E(V-R) = 0.35$ and $E(R-I) = 0.4$. To check the consistency with our data and estimate the values of interstellar extinction for the Geminga emission, we analysed the results of our photometry for the bluest point-like field objects, which are definitely detected in the images taken with the B or V filter, with the acquisition of normal level (within the linear part of the detector dynamic range) in the R and I images (Table 5). The reddest stars (saturated even

at short exposures) were not considered. The colour-magnitude diagrams V *vs* V−R and R *vs* R−I obtained are shown in Fig. 3. For comparison we show there the relation for unreddened stars of the main sequence at distances of 0.5, 1 and 5 kpc. The values of colour indices for most of the field objects are as those of the main sequence stars (Table 7) of spectral type F and later, reddened up to $A_V \sim 1.5$, that is in agreement with the above upper limits. The particular position of Geminga in the colour-magnitude diagrams and its unusual colours confirm the unique nature of this object. Compared with the colours of the field objects they are evidence of insignificant interstellar reddening of the Geminga emission, which is explained by the small distance (~ 160 pc) of this neutron star from the Sun. Making use of the neutral hydrogen column density, $(0.86{-}1.34) \times 10^{20}$cm^{-2}, obtained by Halpern & Wang (1997) from spectral fits of the X-ray data of Geminga, and of the relation between colour excess and N_H, found to be equal to $N_H/A_V = 4.8 \times 10^{20}$cm^{-2}mag^{-1} (Bohlin et al., 1978),

Table 7: *Colour indices for the main sequence stars (Bessel, 1990)*

	O	B3	B5	B8	A0	A5	F0	F5	G0
B−V	-0.326	-0.193	-0.139	-0.068	-0.012	0.128	0.311	0.411	0.575
V−R	-0.158	-0.073	-0.032	-0.024	0.001	0.063	0.197	0.27	0.352
R−I	-0.172	-0.09	-0.066	-0.044	-0.002	0.077	0.22	0.266	0.363
	G5	K0	K3	K5	K7	M0	M2	M4	M5
B−V	0.654	0.823	0.974	1.182	1.382	1.444	1.479	1.513	1.703
V−R	0.388	0.461	0.582	0.733	0.839	0.886	0.99	1.092	1.191
R−I	0.358	0.392	0.497	0.626	0.761	0.849	1.08	1.36	1.571

we obtained $E(B - V) = 0.018$–0.028. Thus, the correction of the Geminga magnitudes and colours for interstellar extinction appears to be negligible in comparison with the photometry accuracy. In case the estimates of $E(B - V)$ in this direction have been lowered due to the uncertainties in the calculated value of N_H, the Geminga colours are even more peculiar.

As has already been mentioned, the profile of G appeared to be of a complicated shape. The ground-based observations do not allow resolving its components. The extended object G' is likely to be a background galaxy. To confirm this, additional studies combined with those over the UV and IR ranges are needed.

3. Discussion

The results of our photometry in B, V and R are in agreement with those of earlier studies of Geminga (Mignani et al., 1998), while the estimate of its I magnitude ($25\overset{m}{.}1 \pm 0.4$) is by more than one magnitude higher as compared to the upper limit ($\geq 26\overset{m}{.}4$) given in the paper mentioned above. This difference is significant despite the poor accuracy of our estimate. The large errors were caused mainly by the high level of the sky background, moderate seeing and insufficient total exposure time. More accurate estimates in the B, R and I bands can be derived provided deeper and better quality images of the field are taken. To study the Geminga spectrum redward, we estimated its flux making use of the infrared data obtained with NICMOS/HST (Harlow et al., 1998) through filters F110W and F160W. For detailed description of the reduction see Koptsevich et al. (2001).

The broad-band spectrum of the Geminga pulsar, summarizing all the data published (see Mignani et al., 1998; Koptsevich et al., 2001) and our results (filled circles), is shown in Fig. 4. The dashed line corresponds to the Rayleigh-Jeans part of the blackbody spectrum describing thermal emission of a neutron star with a 10 km radius and a temperature of $5.77 \cdot 10^5$ K, which is the result of the spectral fit of the ROSAT X-ray data (Halpern & Ruderman, 1993). It can be seen that redward of 6000Å

the Geminga flux differs from the thermal spectrum, which allows us to speak about the nonthermal nature of the Geminga emission in this range.
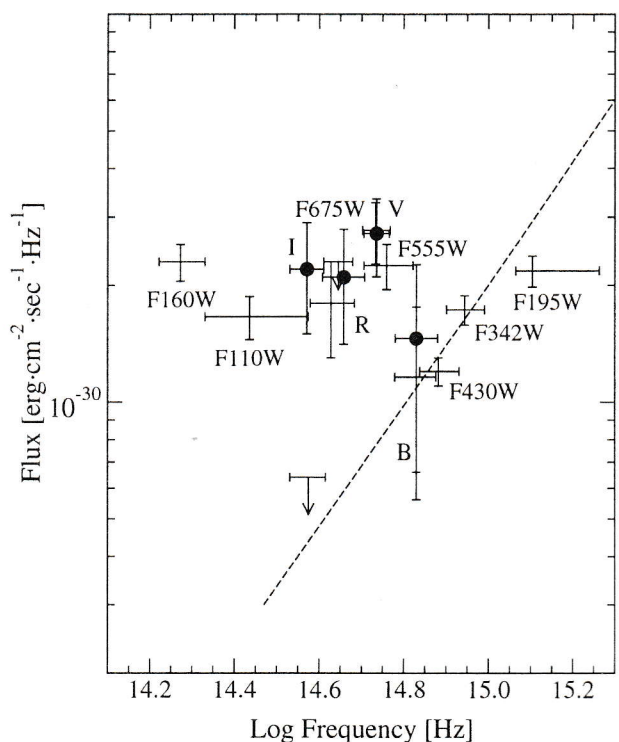

Figure 4: *Broad-band spectrum of Geminga summarizing near-UV (Bignami et al., 1996), optical (Mignani et al., 1998; this work) and infrared (Koptsevich et al., 2001) data. Our results are shown in filled circles. Dashed line corresponds to the Rayleigh-Jeans part of the blackbody fit of ROSAT data of Geminga for a neutron star of 10 km radius and a temperature of $5.77 \cdot 10^5$ K (Halpern and Ruderman, 1993).*

The model of the ion cyclotron emission, proposed to explain an excess over the thermal component centred in the V band with the sharp cutoff in the I band shown by previous optical data (Jacchia et al., 1999), could hardly account for the actual spectral distribution of the Geminga optical emission provided by new observations. Our results show rather flat spec-

trum or a slight increase of the Geminga flux toward infrared range. The excess in V due to some unresolved spectral features is still possible but it is much fainter than it was suggested by previous data.

The spectrum of another middle-aged neutron star, PSR B0656+14, shows a similar non-monotonous behaviour (Kurt et al., 1998; Koptsevich et al., 2001). The spectral features observed as excesses in the optical emission of both neutron stars, PSR B0656+14 and Geminga, allow suspicion of their being of the same nature. Probable non-thermal character of the emission of these INS in the red domain suggests an idea to detect an optical emission of older neutron stars at these wavelengths mainly. In this connection it is likely worth to mention about the tentative detection in the R band of the optical counterpart of PSR B0950+08 (Kurt et al., 2000), which is a nearby old neutron star ($\tau \sim 1.7 \times 10^7$ yrs, distance d=280±2.5 pc, by data of Brisken et al., 2000).

Fig. 5 displays broad-band spectra covering the UV–IR range for INS of different ages, the Crab pulsar (Percival et al., 1993; Eikenberry et al., 1997), PSR B0540-69 (Middleditch et al., 1987), the Vela pulsar (Nasuti et al., 1997), PSR B0656+14 (Koptsevich et al., 2001) and Geminga (Mignani et al., 1998; Koptsevich et al., 2001; this work). There are differences in the spectra of middle-aged neutron stars, such as PSR B0656+14 and Geminga, if compared with flat and featureless spectra of young pulsars, which testifies possible evolution of optical emission of INS with age.

To find out a complete picture one needs detailed studies of energy distribution in spectra of neutron stars of different ages. Spectral observations of such faint ($\geq 25^m$) objects even of a low resolution and subsequent data reduction is extremely hard job (see Martin et al., 1998), especially in the red domain, with strong night sky emission lines and fringe patterns occuring in CCD observations. Supposing possible spectral feature in the optical emission of INS to be rather broad (FWHM ~ 100Å), one may find promising observations with a set of middle-band filters (Afanasiev et al., 2000) using the technique proposed to study extragalactic objects of high red shifts, which gives quite a detailed spectrum of the object under study. Apart from the 6 m telescope, observations using such a method are possible with the telescope SUBARU (Hayashino et al., 2000). The photometric studies of neutron stars of different ages with a high time resolution are also by far of importance. If the pulsed component is detected, it will give a new piece of information about the optical emission nature.
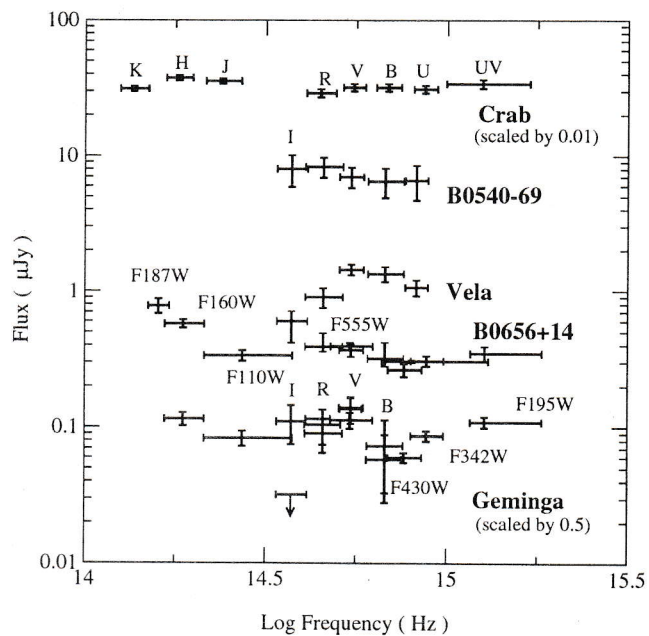
Figure 5: *Broad-band spectra covering the UV–IR range for INS of different ages, from the youngest ($\tau \sim 10^3$) Crab pulsar (at the top of the panel) to much older ($\tau \sim 10^5$) Geminga (at the bottom). The spectral evolution with age can be retraced.*

References

Afanasiev V.L., Dodonov S.N., Moiseev A.V., 2000, http://www.sao.ru/ moisav/scorpio/scorpio.html

Bessel M.S., 1990, Publ. Astr. Soc. Pacific, **102**, 1181

Bignami G.F., Caraveo P.A., Mignani R., Edelstein J., Bowyer S., 1996, Astrophys. J., **456**, L111

Bignami G.F., Caraveo P.A., Paul J.A., 1987, Astron. Astrophys., **202**, L1

Brisken W.F., Benson J.M., Beasley A.J., Fomalont E.B., Goss W. M., Thorsett S.E., 2000, Astrophys. J., **541**, 959

Bohlin R.C., Savage B.D. & Drake, J.F., 1978, Astrophys. J., **224**, 132

Caraveo P.A., Bignami G.F., Mignani R., & Taff L.G., 1996, Astrophys. J., **461**, L91

Eikenberry S.S., Fazio G.G., Ransom S.M., Middleditch J., Kristian J., Pennypacker, C.R., 1997, Astrophys. J., **477**, 465

Fichtel C.E., Hartman R.C., Kniffen D.A., Thompson D.J., Ogelman H., Ozel M.E., Tumer T., Bignami G.F., 1975, Astron. J., **198**, 163

Fukugita M., Shimasaku K., and Ichikawa, T., 1995, Publ. Astr. Soc. Pacific, **107**, 945

Halpern J.P. & Holt S. S., 1992, Nature, **357**, No. 6375, 222

Halpern J.P. & Ruderman M., 1993, Astrophys. J., 415, 286

Halpern J.P. & Tytler D., 1988, Astrophys. J., **330**, 201

Halpern J.P. & Wang, Y.-H., 1997, Astrophys. J., **477**, 905

Harlow J.J.B., Pavlov G.G., Halpern J.R., 1998, AAS Meeting, 193, **No. 41.07**

Hayashino T., Taniguchi Yo., Yamada T., et al., 2000, Subaru Telescope Preprint and Reprint Series, **No. 100**, 21

Jacchia A., De Luca F., Lazzio E., Caraveo P.A., Mignani R.P., Bignami G.F., 1999, Astron. Astrophys., **343**, 497

Koptsevich A.B., Pavlov G.G., Zharikov S.V., Shibanov Yu.A, Sokolov V.V., Kurt V.G., 2001, Astron. Astrophys., **370**, 1004

Kuz'min A.D., Losovskii B.Ya., 1997, Pis'ma Astron. Zh., **23**, 323

Kurt V.G., Sokolov V.V., Zharikov S.V., Pavlov G.G., Komberg B.V., 1998, Astron. Astrophys., **333**, 547

Kurt V.G., Komarova V.N., Fatkhullin T.A., Koptsevich A.B., Sokolov V.V., Shibanov Yu.A., 2000, Bull. Spec. Astrophys. Obs., **49**, 5

Landolt A.U., 1992, Astron. J., **104**, 340

Malofeev V.M. and Malov O.I., 1997, Nature, **389**, 697

Martin C., Halpern J.P., Schiminovich D., 1998, Astrophys. J., **494**, L211

Meyer R.D., Pavlov G.G., Mezharos P., 1994, Astron. J., **433**, 265

Middleditch J., Pennypacker C.R., & Burns M.S., 1987, Astrophys. J., **315**, 142

Mignani R., Caraveo P.A. & Bignami G.F., 1994, Messenger, **76**, 32

Mignani R., Caraveo P.A. & Bignami G.F., 1998, Astron. Astrophys., **332**, L37

Malofeev V.M., Malov O.I., 2000, Astron. Zh., **77**, 52

Nasuti F.P., Mignani R., Caraveo P.A., & Bignami G.F., 1997, Astron. Astrophys., **323**, 839

Percival J.W., Biggs J.D., Dolan J.F., et al., 1993, Astrophys. J., **407**, 276

Shearer A., Golden A., Harfst S., et al., 1998, Astron. Astrophys., **335**, L21

Shitov Yu.P., Pugachev V.D., 1997, New Astronomy, **3**, 101

Schlegel D., Finkbeiner D., & Davis M., 1998, Astrophys. J., **500**, 525

Yakovlev D.G., Levenfish K.P., Shibanov Yu.A., 1999, Uspekhi Physicheskikh Nauk (in Russian), **42**, 825